Nonclassical Crystallization: Mesocrystals and Morphology Change of $CaCO_3$ Crystals in the Presence of a Polyelectrolyte Additive

Tongxin Wang, Helmut Cölfen,* and Markus Antonietti*

Max Planck Institute of Colloids and Interfaces, Colloid Chemistry, Research Campus Golm, Am Mühlenberg, D-14424 Potsdam, Germany

E-mail: Coelfen@mpikg-golm.mpg.de; Pape@mpikg-golm.mpg.de

Crystallization control is one of the most important techniques of preparation, purification, and application of solid substances, making it an intensely studied field. As nucleation and growth are very sensitive processes, crystallization is usually controlled by various additives. Besides conventional crystallization, there are also nonclassical pathways of crystallization via colloidal intermediates and mesoscale transformation,[1−3] in which crystalline structures are constructed and/or transformed from larger units instead of single ions. These mesoscale processes are highly sensitive to a polymer additive in a variety of ways,[1] such that the accurate prediction of particle morphology is still impossible. In addition, crystals can be assembled from nanoscopic building units in an almost perfect three-dimensional orientation to form so-called mesocrystals, exhibiting well-faceted outer surfaces. In the case of inorganic minerals,[4−7] these typically fuse to single crystals, likely as a result of high lattice energy, whereas in organic crystals[8] they can be isolated. Crystallization and morphological control of $CaCO_3$ as a scientifically and industrially important mineral system have attracted extensive attention for decades and were recently reviewed.[9,10] Many materials including Langmuir monolayers,[11,12] self-assembled films,[13,14] bio-[15,16] or synthetic[17,18] macromolecules, low molecular weight compounds,[19,20] and others were used effectively to control $CaCO_3$ morphologies and polymorphs.

Here, we present a simple system of calcite paired with polystyrene sulfonate (PSS), which undergoes mesocrystal formation. Appropriate concentration adjustment of both partners allows broad, systematic variation of the mesocrystal morphology that demonstrates long-range interactions. Moreover, we report that selective coding of nanocrystal surfaces by polymers can not only lead to mesocrystals exposing unusual crystal faces in their superstructure, but also can form self-assembled structures with changed symmetry.

When $CaCO_3$ is crystallized without additives with the applied gas diffusion technique, typical calcite rhombohedra are formed. Addition of minor amounts (0.1 g/L) of PSS leads to two effects. First, the crystalline species become homogeneous in size and morphology as PSS encourages and simplifies nucleation. This is shown by the increased number and decreased size of the particles (data not shown). Second, the crystal surface structure becomes increasingly rough (Figure 1).

The formation of porous crystals and their rough surfaces strongly indicates a change of the crystallization mechanism from ionic growth to mesoscale assembly.[6] That is, PSS not only simplifies nucleation of multiple crystals for mesoscale assembly but also complexes Ca^{2+}, decreasing the free ion concentration and reducing the rate of ionic growth.[21] Thus, a PSS−Ca complex is the primary species in solution. As a consequence, all crystals discussed in this work are constructed by this mesoscale assembly. The existence of amorphous calcium carbonate nanoparticles (density: 1.44−1.58 g/mL from analytical ultracentrifugation, AUC, not shown) in the suboptical size range at the early crystallization stages (from TEM, Figure 2, dynamic light scattering, Supporting Information Figure 2, and AUC, not shown) and ca. 20−30 nm primary calcite building units in the final crystals (from WAXS Scherrer evaluation, Supporting Information Figure 3) and ca. 50 nm from AFM (not shown) provide further evidence for mesoscale assembly[1] from amorphous primary particles[22] to amorphous aggregates with subsequent crystallization and assembly to mesocrystals. In addition, the Brunauer−Emmett−Teller (BET, Supporting Information Figure 1) measurements show that these calcite mesocrystals are highly porous, and all of their surface areas are larger than 260 m^2/g. The size distribution curves calculated from the adsorption branch of nitrogen isotherms show that the sample mesopores have narrow distributions, with maximum pore diameters of between 3 and 10 nm.

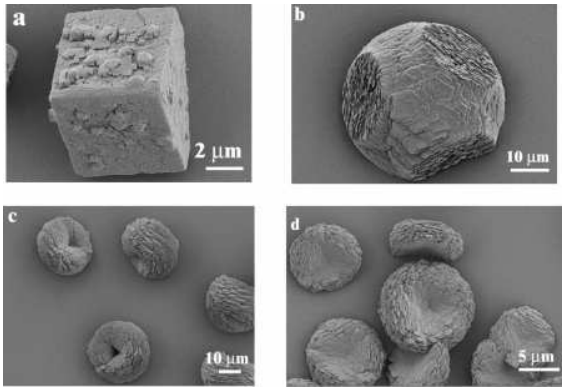

Figure 1. SEMs of calcite mesocrystals obtained on glass slips by gas diffusion reaction after 1 day in a 1-mL solution with different concentrations of Ca^{2+} and PSS. (a) $[Ca^{2+}] = 1.25$ mmol/L, [PSS] = 0.1 g/L. (b) $[Ca^{2+}] = 1.25$ mmol/L, [PSS] = 1.0 g/L. (c) $[Ca^{2+}] = 5$ mmol/L, [PSS] = 0.1 g/L. (d) $[Ca^{2+}] = 5$ mmol/L, [PSS] = 1.0 g/L.

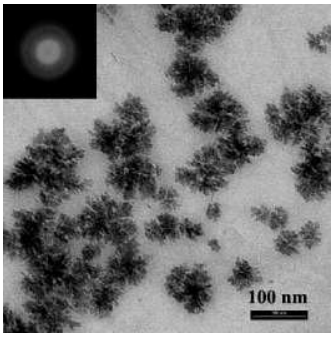

Figure 2. TEM image and the selected area electron diffraction pattern (SAED, inset) showing that the nanoparticles from the early crystallization stage are amorphous. The sample was from a 5-mL solution with $[Ca^{2+}] = 1.25$ mmol/L, [PSS] = 1 g/L after 2 h crystallization.

Also, PSS shows a strong influence on the mesocrystal morphology when Ca^{2+} and PSS concentrations were systematically varied (Figure 1).

At the lowest Ca^{2+} and PSS concentrations of 1.25 mmol/L and 0.1 g/L, respectively (Figure 1a), we still obtain rhombohedral calcite structures, but they are composed of smaller calcite substructures, showing that the polymer influence onto the mutual interaction is weak. Note that the first species already possess rounded corners. Although similar structures with round corners and rough surfaces have been shown previously, they are different from our mesocrystals.[23,24]

Increasing PSS concentration to 1 g/L, but keeping a low Ca^{2+} concentration (1.25 mmol/L, Figure 1b), leads to suppression of nanoparticle assembly along 6 edges out of 12, and the resulting rounded structure has no further resemblance to the primary rhombhedra. The two "rounded" corners are along the [001] direction, as revealed by the absence of double refraction in polarized light microscopy (PLM, Supporting Information Figure 4). Discrimination of the *c*-axis with hexagonal symmetry allows a better understanding of the mesoscale assembly process.

Although exposed (001) faces, constituting either pure cationic or anionic sites (Supporting Information Figure 5), are not usually observed, they have been found, for example, by using additives of sulfonated dye molecules.[25]

In our case, these surfaces are stabilized by multiple Coulombic binding of PSS. However, the active structure shaping is determined by the stacking efficiency of the mesoscale assembly, instead of by preservation of crystal geometry that would indicate ionic crystallization.

The most complicated structures, uniform semiconvex crystalline superstructures, are obtained at the highest Ca^{2+} concentrations of 5 mmol/L (see Figure 1c,d). Astonishingly, the particles change symmetry and are nearly circular in the now structure-determining (001) direction, as revealed by PLM (Supporting Information Figure 4). However, in this perpendicular direction, opposite sides are respectively convex and concave. The lower the polymer concentration is, the more pronounced this asymmetry and the more strongly curved the structures. With decreasing PSS concentration, fewer and larger particles are generated, and the described assembly process finally leads to a central hole (Figure 1c).

The above results show that the porous mesocrystals are composed of nanocrystals with exposed, highly positive (001) faces, ideal for the adsorption of PSS (see also Supporting Information Figure 5). In addition, PLM revealed that these nanocrystals were assembled along the *c*-axis direction to form mesostructures. These morphologies, especially their semiconvex structures, contradict all classical pictures of crystallization based on symmetry encoding in the unit cell,[26] where such a hole should vanish by Ostwald ripening.

The observed morphology can be interpreted in terms of selective PSS adsorption that favors the positive (001) surface. We propose that adsorption by negative species to the opposite face is thus prevented by dielectric interaction throughout the crystal, and that the resulting dipole along the *c*-axis drives the nanoparticle assembly. The observed hole and well-developed opposite side (Figure 1c) are strongly indicative of a long-range dipolar control, where overall negatively charged particles aggregate preferentially at the positive ends of the emerging dipolar superstructures. The full mechanism of this nonclassical crystallization event will be reported in a subsequent study.

In summary, the calcite crystallization in the presence of PSS yielded a family of well-defined mesocrystals (i.e., regular but porous scaffolds composed of well-separated, but almost perfectly three-dimensionally aligned calcite nanocrystals), in contrast to $BaCO_3$ aggregates found with the same PSS but at higher Ba^{2+} concentration.[27] The observed systematic behavior can be explained by simultaneous multiple mode polymer interaction with the crystallization process. PSS strongly binds free calcium ions, shifts the mechanism from ionic growth to mesoscale assembly, and acts as a nucleation agent. It also binds selectively to the otherwise nonexposed (001) calcite face, resulting in mesostructures composed of truncated triangular units instead of the typical rhombohedra. A new effect, dipolar arrangement of primary nanoparticles in the *c*-direction changing mesocrystal morphology, is found at high supersaturation and resulting nucleation burst. Adsorption and dipolar asymmetry might be characteristic for very small polymer-protected particles. In such cases, inner field effects within the crystal cannot be neglected, which is an entirely new aspect of polymer-controlled crystallization processes.

Acknowledgment. We thank the Max Planck Society for financial support and a fellowship for T.X.W. We also thank Dr. Andreas Erbe for DLS, Antje Völkel for AUC, Dr. Jürgen Hartmann for SAED, and Thorsten Brezesinski for BET.

Supporting Information Available: Experimental details, DLS and WAXS data, BET, Cerius^2 computer models of calcite, and PLM images. This material is available free of charge via the Internet at http://pubs.acs.org.

References

(1) Cölfen, H ; Mann, S *Angew. Chem., Int. Ed.* **2003**, *42*, 2350−2365
(2) Jongen, N ; Bowen, P ; Lemaître, J ; Valmalette, J C ; Hofmann, H *J. Colloid Interface Sci* **2000**, *226*, 189−198
(3) Penn, R L ; Banfield, J F *Geochim. Cosmochim. Acta* **1999**, *63*, 1549−1557
(4) Zhan, J H ; Lin, H P ; Mou, C Y *Adv. Mater.* **2003**, *15*, 621−623
(5) Grassmann, O ; Neder, R B ; Putnis, A ; Löbmann, P *Am. Mineral.* **2003**, *88*, 647−652
(6) Judat, B ; Kind, M *J. Colloid Interface Sci.* **2004**, *269*, 341−353
(7) Shevchenko, E V ; Talapin, D V ; Rogach, A L ; Kornowski, A ; Haase, M ; Weller, H *J. Am. Chem. Soc.* **2002**, *124*, 11480−11485
(8) Wohlrab, S ; Pinna, N ; Antonietti, M ; Cölfen, H *Chem.−Eur. J.*, in press; DOI: 10 1002/chem 200400420
(9) Meldrum, F C *Int. Mater. Rev.* **2003**, *48*, 187−224
(10) Kato, T ; Sugawara, A ; Hosoda, N *Adv. Mater.* **2002**, *14*, 869−877
(11) Mann, S ; Heywood, B R ; Rajam, S ; Birchall, J D *Nature* **1988**, *334*, 692−695
(12) Lahiri, J ; Xu, G F ; Dabbs, D M ; Yao, N ; Aksay, I A ; Groves, J T *J. Am. Chem. Soc.* **1997**, *119*, 5449−5450
(13) Kuther, J ; Nelles, G ; Seshadri, R ; Schaub, M ; Butt, H J ; Tremel, W *Chem.−Eur. J.* **1998**, *4*, 1834−1842
(14) Aizenberg, J ; Black, A J ; Whitesides, G M *Nature* **1999**, *398*, 495−498
(15) Belcher, A M ; Wu, X H ; Christensen, R J ; Hansma P K ; Stucky, G D ; Morse, D E *Nature* **1996**, *381*, 56−58
(16) Addadi, L ; Weiner, S *Proc. Natl. Acad. Sci. U.S.A.* **1985**, *82*, 4110−4114
(17) Yu, S H ; Cölfen, H *J. Mater. Chem* **2004**, *14*, 2124−2147
(18) Gower, L B ; Odom, D J *J. Cryst. Growth* **2000**, *210*, 719−734
(19) Mann, S ; Archibald, D D ; Didymus, J M ; Douglas, T ; Heywood, B R ; Meldrum, F C ; Reeves, N J *Science* **1993**, *261*, 1286−1292
(20) Orme, C A ; Noy, A ; Wierzbicki, A ; McBride, M T ; Grantham, M ; Teng, H H ; Dove, P M ; DeYoreo, J J *Nature* **2001**, *411*, 775−779
(21) Sinn, C G ; Dimova, R ; Antonietti, M *Macromolecules* **2004**, *37*, 3444−3450
(22) Addadi, L ; Raz, S ; Weiner, S *Adv. Mater* **2003**, *15*, 959−970
(23) Estroff, L A ; Addadi, L ; Weiner, S ; Hamilton, A D *Org. Biomol. Chem.* **2004**, *2*, 137−141
(24) Grassmann, O ; Löbmann, P ; *Chem.−Eur. J.* **2003**, *9*, 1310−1316
(25) Shan, W ; Wang, B ; Zhang, Y H ; Wu, B Y ; Tang, Y *Chem. Lett* **2004**, *33*, 1248−1249
(26) Wulff, G *Z Krystallogr.* **1901**, *34*, 449−480
(27) Yu, S H ; Cölfen, H ; Xu, A W ; Dong, W F *Cryst. Growth Des.* **2004**, *4*, 33−37

JA045331G